Clockwise Translocation of Microtubules by Flagellar Inner-Arm Dyneins In Vitro

Kenji Kikushima* and Ritsu Kamiya*[†]

*Department of Biological Sciences, Graduate School of Science, The University of Tokyo, Tokyo, Japan; and [†]CREST, Japan Science and Technology Corporation, Kawaguchi, Japan

ABSTRACT   Cilia and flagella are equipped with multiple species of dyneins that have diverse motor properties. To assess the properties of various axonemal dyneins of *Chlamydomonas*, in vitro microtubule translocation by isolated dyneins was examined with and without flow of the medium. With one inner-arm dynein species, dynein *c*, most microtubules became aligned parallel to the flow and translocated downstream after the onset of flow. When the flow was stopped, the gliding direction was gradually randomized. In contrast, with inner-arm dyneins *d* and *g*, microtubules tended to translocate at a shallow right angle to the flow. When the flow was stopped, each microtubule turned to the right, making a curved track. The clockwise translocation was not accompanied by lateral displacement, indicating that these dyneins generate torque that bends the microtubule. The torque generated by these dyneins in the axoneme may modulate the relative orientation between adjacent doublet microtubules and lead to more efficient functioning of total dyneins.

INTRODUCTION

Cilia and flagella produce bending waves based on the sliding between outer-doublet microtubules. The driving force is produced by multiple species of inner-arm and outer-arm dynein heavy chains, each with a AAA^+ ATPase domain (1–4). The presence of multiple dyneins with distinct properties is important for generating a proper beat (5). It is not clear, however, how the total dyneins attached to cylindrically arranged outer doublet microtubules can contribute to the axonemal bending, which occurs in a plane in most organisms.

The motile properties of dyneins have been studied by assaying microtubule gliding over a glass surface coated with a particular species of dynein (6–8). In such in vitro assays, both cytoplasmic dynein and all axonemal dyneins have been shown to translocate microtubules with their plus-ends leading. In addition, some inner-arm dyneins (single-headed dyneins) that contain a single heavy chain rotate microtubules around their long axis during translocation (7,8). Such axial rotation has not been reported for outer-arm dynein or cytoplasmic dynein. The physiological significance of the axial rotation is not known. However, a slight rotation of an outer-doublet microtubule in the axoneme may impose a significant effect on the interaction between various dyneins and the adjacent outer doublet. Therefore, axial rotation may be important for the regulation or coordination of the dynein force generation required for flagellar beating.

In our study, we observed a novel type of microtubule rotation while examining the effects of the flow of the medium on the motile properties of inner-arm dyneins isolated from *Chlamydomonas* flagella. Microtubules translocated by some single-headed inner-arm dyneins on the glass slide tend to continuously change their advancing direction in a clockwise direction and travel in circular tracks. This movement is apparently distinct from that of axial rotation. We propose that the circular translocation occurs because these dyneins produce torques perpendicular to the long axis of the microtubule and that the particular dynein molecule interacting with the advancing plus end of a microtubule bends the microtubule to the right. Torque generation by dyneins in the axoneme may modulate the relative orientation between adjacent microtubules, possibly leading to more efficient force production for beating by various dynein molecules.

MATERIALS AND METHODS

Dyneins were isolated from the axonemes of *Chlamydomonas reinhardtii oda1* (a mutant lacking outer-arm dynein) by extraction with 0.6 M KCl. The high-salt extract was dialyzed against HMDE (30 mM Hepes, 5 mM MgSO$_4$, 1 mM DTT, 1 mM EGTA) and fractionated into seven inner-arm subspecies (*a* to *g*) by HPLC on a MonoQ column (8) (Fig. 1). Tubulin was purified from porcine brain using polymerization-depolymerization cycles and phosphocellulose chromatography (9). Microtubules were prepared by polymerizing the tubulin at 37°C and stabilized by dilution of the sample into HMDE containing 10 μM Taxol.

In vitro motility assays were carried out based on previous studies (8,10,11). Each dynein sample (0.05 mg/ml) was introduced into a flow chamber (see below) and incubated for 3 min, followed by introduction of HMDE containing 2 mg/ml bovine serum albumin. After microtubules in HMDE were introduced, in vitro translocation was initiated by perfusing the chamber with HMDE containing 10 μM Taxol with appropriate concentrations of ATP and ADP. ADP was included because it has a stimulatory effect on the motility generated by inner-arm dyneins (11). To avoid the effects of collisions between microtubules, we used microtubule samples at a concentration of ~2 μM, which is fivefold lower than that which we usually use for in vitro motility assay studies.

The flow chamber used for observation was constructed using a glass slide, a coverslip, and a pair of spacers made of plastic adhesive tape. The internal size of the chambers was 18 × 5 × 0.08 mm. The glass slide used
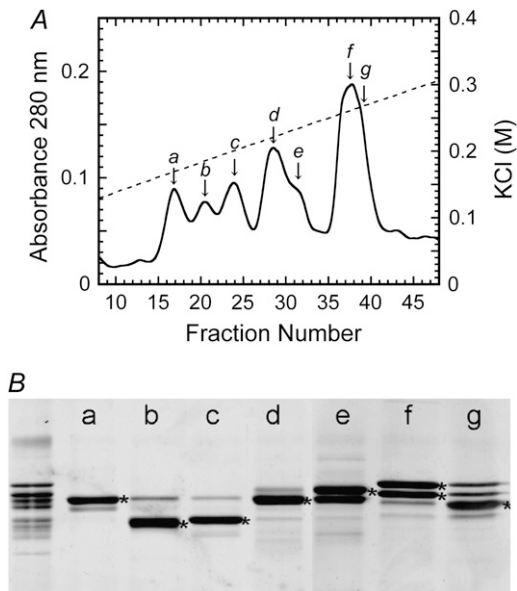
FIGURE 1 Separation of inner-arm dynein subspecies. (A) Inner-arm dyneins, extracted from the *oda1* axoneme, were separated into seven subspecies, *a–g*, by chromatography on a MonoQ anion-exchange column. (*Solid line*) Absorbance at 280 nm. Dotted line, KCl concentration. (B) The SDS-PAGE pattern of the peak fractions, showing the dynein heavy-chain bands. The leftmost lane is the original high-salt extract. The heavy chians of species *a–g* are marked with asterisks.

was Matsunami No. 1 (Tokyo, Japan) washed with SDS, rinsed with distilled water, and air-dried. In experiments to examine the effect of the conditions of glass surfaces, glass slides were also used that had been immersed in 0.1 M HCl or in 0.1 M NaOH for 24 h, or silicone-coated with Sigmacoat (Sigma Chemical, St. Louis, MO). However, microtubules did not attach to the glass slides treated with NaOH or Sigmacoat. The coverslip was slightly bent on one side by heating, so as to attach a hypodermic needle used as the entrance port for perfusion. The side with the needle was sealed with silicon rubber so that the medium did not leak out. Flow was applied by perfusing the chamber with a buffer solution using a peristaltic pump and a piece of filter paper placed on the opposite side of the chamber. The direction of flow was monitored by the small bubbles present in the medium. At the most frequently used setting, the flow rate was calibrated to be 103 μl/min. If we assume that the medium flow is parallel to the wall of the chamber and behaves as Poiseuille flow with a viscosity identical to that of water $(8.9 \times 10^{-4}$ Pa·s), then the local flow speed of the medium y μm above the glass slide is given by $u(y)$ $(\mu$m/s$) = 4.0 \times y(80 - y)$. Thus, the maximum flow speed, on the midplane between the two glass surfaces, is $u(y = 40 \ \mu$m$) = 6.4$ mm/s. If microtubules glide 30 nm above the glass slide, the flow speed they experience is $u(y = 30 \ nm) = 9.6 \ \mu$m/s.

Movements of microtubules were observed with an upright dark-field microscope equipped with a 100-W mercury arc lamp and an SIT camera (Hamamatsu Photonics, Hamamatsu City, Japan). The images were recorded on videotape and computer analyzed. The average radius of curvature in a gliding track was obtained by averaging local curvatures, which were determined from three successive points (1 s apart) on the track, over the entire track.

RESULTS AND DISCUSSION

Effects of medium flow on the direction of microtubule translocation

To obtain clues to the functional differences among various axonemal dyneins, we examined the effects of the medium
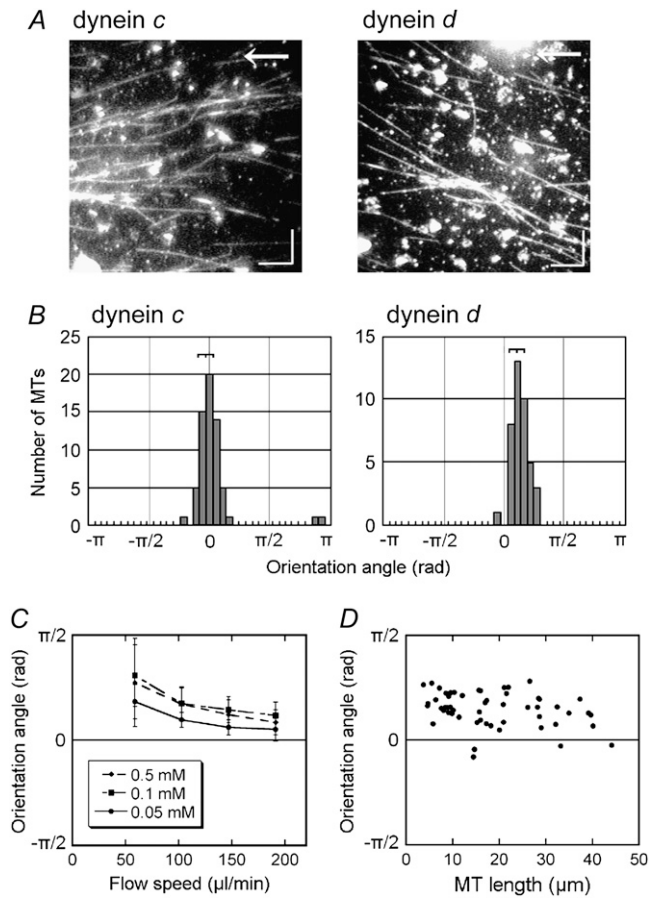

FIGURE 2 Effects of flow on the direction of microtubule translocation. (A) Dark-field images of microtubules on glass surfaces covered with dynein *c* or *d*, taken 3 min after application of shear flow (103 μl/min). Arrows indicate the direction of flow. (*Bars*) 10 μm. (B) Distribution of the angles between the direction of flow and the microtubule (orientation angle) at 3 min after initiation of the flow. The angle is defined as positive when the microtubule glides in a right-handed direction to the flow. The orientation angles were -0.1 ± 0.2 rad ($n = 61$) for dynein *c* and 0.4 ± 0.2 rad ($n = 40$) for dynein *d*. (C) Relation between the orientation angle ($\pm$ SD) and the flow speed in the presence of various concentrations of ATP (0.05–0.5 mM) and 0.1 mM ADP in dynein *d*-translocated microtubules. (D) Dependence of the orientation angle on microtubule length in dynein *d*-translocated microtubules. Flow speed, 103 μl/min. The medium contained 0.5 mM ATP and 0.1 mM ADP in *A*, *B*, and *D*.

flow on the in vitro microtubule translocation by isolated dyneins. Inner-arm dyneins extracted from *Chlamydomonas oda1* axonemes were separated by ion-exchange chromatography into seven species (dyneins *a–g*) (8) (Fig. 1) and used to coat the glass slide in a flow chamber. First, two species of single-headed dyneins, dynein *c* and dynein *d*, were examined. With either dynein, microtubules glided on the dynein-coated glass surface in apparently random directions when the solution became settled after introduction of microtubules and ATP into the chamber. When microtubules were subjected to flow produced by continuous perfusion with the ATP-containing medium, they became oriented to the direction of the flow and tended to move downstream. This behavior of microtubules under flow is similar to that
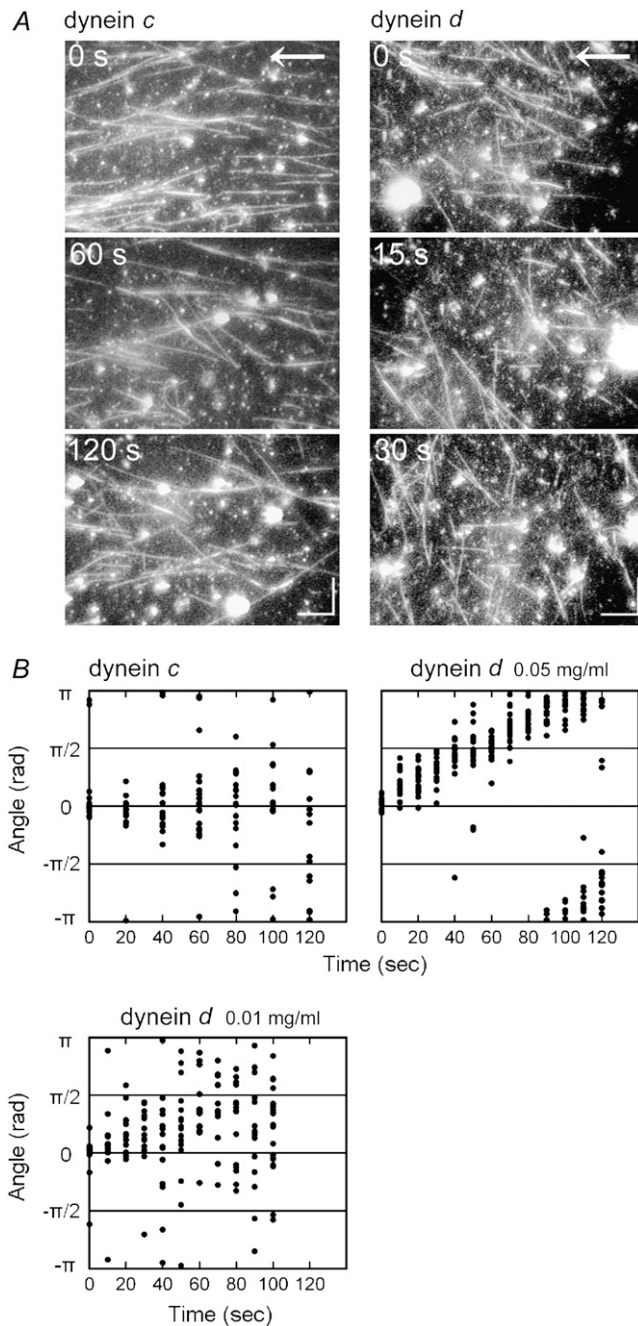
reported for a kinesin-based in vitro motility system (12), although the polarity of the microtubules in the dynein system is opposite that of the kinesin system. On close examination of the orientation after ≥3 min of perfusion, however, we noticed a striking difference between dynein *c* and dynein *d* (Fig. 2, *A* and *B*). In the dynein *c* motility system, the microtubule orientation was nearly parallel to that of the flow, and the average angle between the microtubule long axis and the flow (the orientation angle) was almost zero. In the dynein *d* motility system, in contrast, microtubules were not parallel to the flow but were skewed to the right. The orientation angle in the dynein *d* system depended on both the velocity of the flow and the ATP concentration but did not
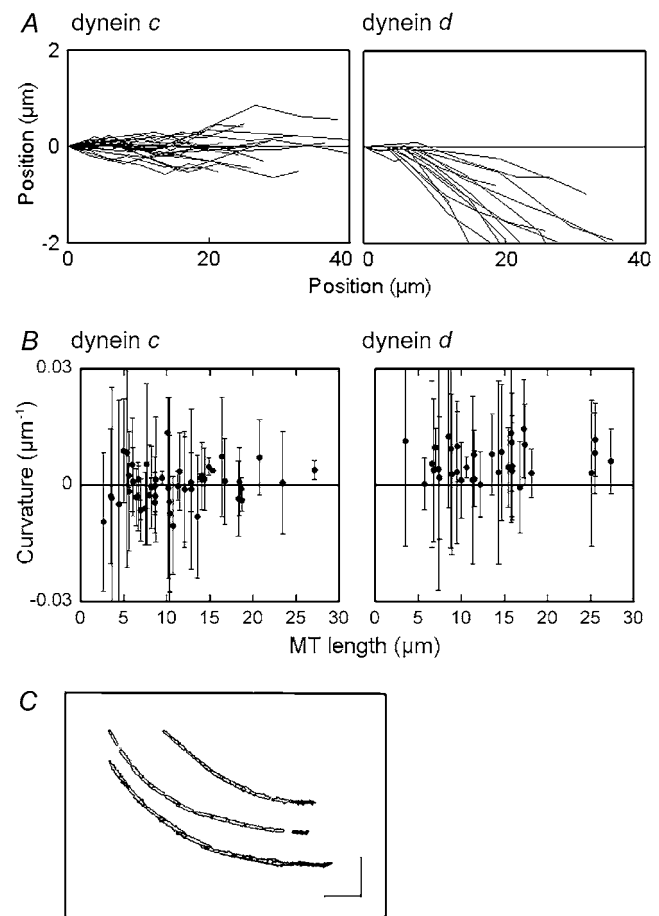

FIGURE 3 Change in the microtubule orientation after removal of flow. (*A*) Successive images of microtubules after cessation of perfusion. Arrows indicate the direction of flow. Bars: 10 μm. The medium contained 0.1 mM ATP and 0.1 mM ADP. A movie of the images with dynein *d* is available (Video 1). (*B*) Change in the microtubule orientation after removal of flow on glass surfaces coated with dynein *c* or *d* (density 0.05 mg/ml or 0.01 mg/ml). The gliding velocity of microtubules translocating on dynein *d* was 2.9 ± 0.4 μm/s ($n = 20$) and 3.2 ± 0.6 μm/s ($n = 20$) for 0.05 mg/ml or 0.01 mg/ml dynein, respectively. The data were fit to a linear function, and the change in microtubule orientation with 0.01 mg/ml dynein was 0.0087 rad/s, which corresponds to a radius of 363 ± 69 μm, ~3.5-fold larger than the radius measured for 0.05 mg/ml dynein (see Table 1). ATP, 0.5 mM; ADP, 0.1 mM.

FIGURE 4 Tracking of individual microtubules in the absence of flow. (*A*) Gliding tracks of individual microtubules translocating on inner-arm dynein *c* (*left*) and inner-arm dynein *d* (*right*) in the absence of flow. Each gliding track was recorded by tracking the location of the advancing plus end of a microtubule at 1-s intervals for 10 s. (*B*) Relation between the microtubule length and average curvature (± SD) in each gliding track on glass surfaces coated with dynein *c* or dynein *d*. The average curvature was determined by averaging local curvatures, which were determined from three successive points on the track separated by 1 s, over the entire length of the track produced by tracking for 10 s. (*C*) Examples of gliding tracks for three microtubules on dynein *d*-coated glass. These tracks were drawn by superimposing successive images taken every 1 s for 12 s. The first images are shown in black. (*Bars*) 10 μm. The medium contained 0.5 mM ATP and 0.1 mM ADP.

show a significant dependence on the microtubule length (Fig. 2, *C* and *D*).

When the flow was stopped, the microtubule orientation was gradually randomized in both the dynein *c* and dynein *d* motility systems. In this postflow randomization, the orientation of many microtubules translocated by dynein *d*, but not dynein *c*, displayed a striking clockwise rotation (Fig. 3 and see also the Supplementary Material, Movie S1). These observations suggest that the orientation angle of microtubules on the dynein *d*-coated glass under the flow is determined by the balance between some active bending moment produced by the dynein and the bending moment produced by the viscous force acting on the microtubule.

Tracks of translocating microtubules in the absence of flow

The above observations imply that individual microtubules, when translocating on dynein *d*-coated glass slides, also tend to turn continuously toward the right in the absence of flow, whereas microtubules translocating on dynein *c*-coated glass slides do not. To confirm this possibility, we tracked the movement of individual microtubules by plotting the position of the advancing plus-end of the microtubule for ~10 s. With dynein *d*, the tracks displayed a right-handed skewing from the initial position, whereas with dynein *c*, deviations from the original direction were almost equally distributed between left-handed and right-handed skewing (Fig. 4 *A*). The average curvature in each gliding track, measured by averaging local curvature, was almost zero for dynein *c* ($-0.0002 \pm 0.005 \ \mu m^{-1}$, $n = 51$; all data are represented as mean $\pm$ SD), and was clearly nonzero for dynein *d* ($0.006 \pm 0.004 \ \mu m^{-1}$, $n = 37$) (Fig. 4 *B*). The average curvature did not appear to depend on the length of the microtubule, although the standard deviation was larger in shorter microtubules (Fig. 4 *B*). Therefore, dynein *d* causes microtubules to turn to the right in the absence of flow.

Superimposition of successive images of microtubules gliding on a dynein *d*-coated glass slide showed that each microtubule advanced on a single arc-shaped track for its entire length (Fig. 4 *C*). The circling movement, therefore, is not accompanied by any sideways rolling (lateral displacement) of the microtubules, although dynein *d* is known to be capable of axial rotation (8). Axial rotation without

sideways rolling has been observed with *Tetrahymena* 14 S dynein (7).

Factors that affect the microtubule circling

To characterize the microtubule circling caused by dynein *d*, we examined several factors that might affect the movement. First, we examined the conditions of the glass surface (see Materials and Methods) and the medium. The conditions of the glass surface did not significantly influence the circling as long as microtubule translocation took place. When the assays were performed in a solution containing 50 mM K-acetate, i.e., the condition used for reactivating axonemal beating (13), the microtubules tended to detach from the glass surface after a short episode of circling. However, in this case, we also observed similar clockwise turning of the microtubule during translocation on dynein *d*-coated glass slides. In contrast, microtubules never showed circling on dynein *c*-coated glass slides.

Second, we examined the relation between forward translocation and the circling. The translocation velocity was altered by changing the concentrations of ATP and ADP, both of which have been shown to modulate dynein motor activity (10,11). Under the conditions employed, the translocation velocity varied from $1.4 \pm 0.2 \ \mu m/s$ to $2.9 \pm 0.4 \ \mu m/s$, but the radius of curvature of the circular movement was always close to 100 μm (Table 1). Therefore, the right-handed skew in microtubule translocation appears to be tightly coupled to the translational movement. This suggests that the microtubule circling is caused by an intrinsic feature of the motor activity of dynein *d*.

Finally, we examined the density of dynein molecules on the glass surface. At dynein concentrations lower than 0.01 mg/ml, microtubules were attached to the glass surface only for a short time, and it was difficult to measure the curvature of the microtubule tracks. At 0.01 mg/ml, which is five-fold lower than the concentration used in the experiments described above, the radius of curvature increased ~3.5-fold ($363 \pm 69 \ \mu m$), but the translocation velocity was very similar to the experiments conducted at the higher dynein concentration (0.01 mg/ml, $3.2 \pm 0.6 \ \mu m/s$; 0.05 mg/ml, $2.9 \pm 0.4 \ \mu m/s$) (Fig. 3 *B*). Thus, the microtubules undergo a sharper turn when interacting with a greater number of dyneins. Because the curvature depended on the dynein

TABLE 1 Radius of curvature of microtubule gliding tracks on dynein *d*-coated glass slides in the presence of various concentrations of nucleotides

Nucleotide conditions (mM)		0.1	0.5	1.0	0.1	0.1	0.1	0.1
	[ATP]	0.1	0.5	1.0	0.1	0.1	0.1	0.1
	[ADP]	0.1	0.1	0.1	0	0.1	0.4	0.7
Change in orientation a (rad/s)		0.025	0.029	0.021	0.032	0.023	0.016	0.013
Gliding speed v ($\mu m/s$)[†]		2.4 (0.4)*	2.9 (0.4)	2.2 (0.6)	2.7 (0.4)	2.5 (0.6)	2.0 (0.4)	1.4 (0.2)
Radius of the curvature $r = v/a$ (μm)		96 (16)	100 (13)	105 (29)	85 (13)	109 (26)	125 (25)	108 (15)

*Numbers in parentheses are standard deviations.

[†]Gliding velocities of ~15 microtubules were measured for each condition.
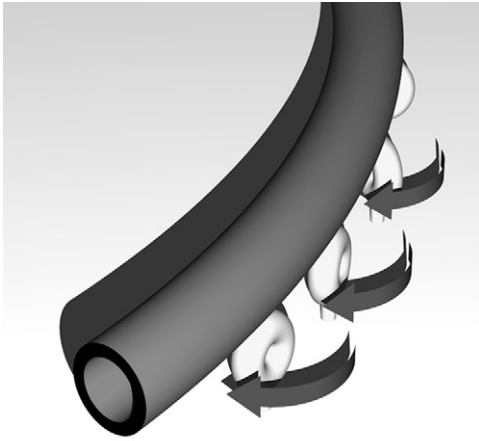
FIGURE 5 Model to explain the right-handed microtubule circling on a dynein-coated surface. All dyneins are assumed to generate torque, but in the middle of a microtubule, the torque is canceled out by the presence of other dyneins bound to the microtubule. Only the dyneins interacting with the advancing front of the microtubule can bend it to the right. The leading end of the microtubule is bent each time it encounters a dynein; thus, the microtubule advances on a curved track. The trailing part of the microtubule is also curved because it remains associated with the dynein molecules that previously interacted with the plus-end portion of the microtubule and bent it. These dyneins are also producing torque but not bending the microtubule.

density but not on the length of the microtubule (Fig. 2 *D*), the curvature must be determined by the number of dynein molecules that interact with a unit length of a microtubule. A simple explanation is that all dynein *d* molecules generate torque in addition to longitudinal gliding force, and the particular dynein interacting with the advancing plus end of the microtubule bends the microtubule to the right and changes the direction of microtubule gliding. Such a torque could be generated if the direction of the power stroke of individual dynein is skewed to the right with respect to the long axis of the microtubule, and the dynein stays on the microtubule after force generation. The dynein molecules interacting with the trailing part of the microtubule also generate torque, but these forces are canceled out by the additional dyneins bound to the microtubule (Fig. 5). With a higher dynein density, a microtubule will make a steeper turn because it undergoes bending more frequently during advancement of the microtubule end.

Inner-arm dynein *g* also displays microtubule circling

Experiments with other dyneins indicated that inner-arm dynein *g* displays a similar clockwise translocation of microtubules, whereas other inner-arm and outer-arm dyneins do not. In experiments with dynein *g* under constant flow, microtubules tended to glide at a shallow right angle to the flow (Fig. 6, *A* and *B*), as observed with dynein *d*. After the removal of flow, each microtubule circled clockwise, making a track with a radius of curvature of ~240 μm (Fig. 6 *C*), which remained almost constant at different nucleotide concentrations (data not shown).

Implications for the mechanism of axonemal beating

The observations described above indicate that each microtubule is bent to the right as it advances on a surface coated with dynein *d* or dynein *g*. Although the arrangement of these dyneins on the outer doublet microtubules in the axoneme and that on the glass surface should differ significantly, the characteristic movements may well perform some important function in the axoneme.

If we assume that 10% of all dynein molecules in the chamber were bound to the glass surface in a functionally active manner (14), the dynein concentration on the surface is 500 dyneins/μm^2 under the conditions we employed. If each dynein could interact with a microtubule located within 20 nm from it, the mean distance between microtubule-bound dyneins is estimated to be 100 nm (15). This value is close to the spacing of dynein *d* on the outer doublet microtubule within the axoneme. The curvature of $(100\ \mu m)^{-1}$ might be negligibly small compared with the maximal curvature observed in the *Chlamydomonas* flagellum $(\sim 2\ \mu m)^{-1}$, and it thus seems unlikely that the microtubule bending itself directly contributes to the gross bending of the axoneme. However, we must bear in mind that, unlike in vitro experiments where the dyneins are attached to a solid surface, dyneins in the axoneme are attached to elastic microtubules, in which the torque generated by dyneins interacting with trailing part of the microtubule is also effective to bend outer doublets. The torque generated by the several tens of dynein
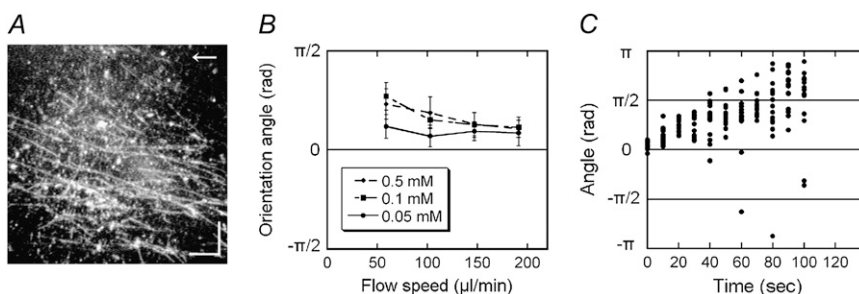

FIGURE 6 Microtubule orientation in experiments using dynein *g*. (*A*) Dark-field images of microtubules translocating under shear flow. Arrow, the direction of flow. Flow speed, 103 μl/min. ATP, 0.5 mM; ADP, 0.1 mM. Bars, 10 μm. (*B*) Relation between the orientation angle and the flow speed at various concentrations of ATP (0.05–0.5 mM). ADP, 0.1 mM. (*C*) Change in the microtubule orientation after removal of flow. ATP, 0.5 mM; ADP, 0.1 mM.

d and *g* molecules present within a single bend might well modulate the relative orientation between two adjacent outer doublet microtubules and potentially lead to more efficient force generation by dynein molecules in the axoneme. The diameter of the axoneme has been shown to increase at the crest of the bending region, indicating that the axoneme undergoes a structural distortion during the beat cycle, which may regulate the interaction between dynein and the outer doublet (16). The torque generated by inner-arm dyneins may also contribute to such distortion of the axoneme. Quantification of the torque generated by a single dynein and an experiment-based assessment of how the torque influences flagellar motility remain important subjects for future studies.

SUPPLEMENTARY MATERIAL

To view all of the supplemental files associated with this article, visit www.biophysj.org.

REFERENCES

1. Neuwald, A. F., L. Aravind, J. L. Spouge, and E. V. Koonin. 1999. AAA$^+$: a class of chaperone-like ATPases associated with the assembly, operation, and disassembly of protein complexes. *Genome Res.* 9:27–43.

2. King, S. M. 2000. AAA domains and organization of the dynein motor unit. *J. Cell Sci.* 113:2521–2526.

3. Vale, R. D. 2000. AAA proteins. Lords of the ring. *J. Cell Biol.* 150: F13–F19.

4. Burgess, S. A., and P. J. Knight. 2004. Is the dynein motor a winch? *Curr. Opin. Struct. Biol.* 14:138–146.

5. Kamiya, R. 2002. Functional diversity of axonemal dyneins as studied in *Chlamydomonas* mutants. *Int. Rev. Cytol.* 219:115–155.

6. Paschal, B. M., S. M. King, A. G. Moss, C. A. Collins, R. B. Vallee, and G. B. Witman. 1987. Isolated flagellar outer arm dynein translocates brain microtubules in vitro. *Nature.* 330:672–674.

7. Vale, R. D., and Y. Y. Toyoshima. 1988. Rotation and translocation of microtubules in vitro induced by dyneins from *Tetrahymena* cilia. *Cell.* 52:459–469.

8. Kagami, O., and R. Kamiya. 1992. Translocation and rotation of microtubules caused by multiple species of *Chlamydomonas* inner-arm dynein. *J. Cell Sci.* 103:653–664.

9. Shelanski, M. L., F. Gaskin, and C. R. Cantor. 1973. Microtubule assembly in the absence of added nucleotides. *Proc. Natl. Acad. Sci. USA.* 70:765–768.

10. Yagi, T. 2000. ADP-dependent microtubule translocation by flagellar inner-arm dyneins. *Cell Struct. Funct.* 25:263–267.

11. Kikushima, K., T. Yagi, and R. Kamiya. 2004. Slow ADP-dependent acceleration of microtubule translocation produced by an axonemal dynein. *FEBS Lett.* 563:119–122.

12. Stracke, R., K. J. Böhm, J. Burgold, H. J. Schacht, and E. Unger. 2000. Physical and technical parameters determining the functioning of a kinesin-based cell-free motor system. *Nanotechnology.* 11:52–56.

13. Bessen, M., R. B. Fay, and G. B. Witman. 1980. Calcium control of waveform in isolated flagellar axonemes of *Chlamydomonas*. *J. Cell Biol.* 86:446–455.

14. Sakakibara, H., H. Kojima, Y. Sakai, E. Katayama, and K. Oiwa. 1999. Inner-arm dynein *c* of *Chlamydomonas* flagella is a single-headed processive motor. *Nature.* 400:586–590.

15. Duke, T., T. E. Holy, and S. Leibler. 1995. Gliding assays for motor proteins: A theoretical analysis. *Phys. Rev. Lett.* 74:330–333.

16. Lindemann, C. B., and D. R. Mitchell. 2007. Evidence for axonemal distortion during the flagellar beat of *Chlamydomonas*. *Cell Motil. Cytoskeleton.* 64:580–589.